Romanian Reports in Physics, Vol. 67, No. 4, P. 1447–1456, 2015

Dedicated to
International Year of Light 2015

SINGLE PHOTON DETECTING SYSTEM

A. RUSU, L. RUSU, L. SERBINA

[1] Horia Hulubei National Institute for R&D in Physics and Nuclear Engineering, IFIN-HH,
30 Reactorului Street, P.O. BOX MG-6, Bucharest – Magurele, Romania,
E-mails: alrusu@nipne.ro, lucian_ru@yahoo.com, serbina@ nipne.ro

Received September 28, 2015

Abstract. Experiments using entangled photons and their applications require the detection of extremely weak light beams: the incoming photons arrive to the detector one at a time. Visible spectrum single photon detection is a challenging problem because the photon energy can produce only one electron-hole pair and such a signal is less than the sum of the intrinsic noise of the semiconductor detector and the associated electronics. Nevertheless, a free electron can initiate an avalanche discharge within an avalanche photodiode (APD), reversely biased at a value slightly higher than its breakdown voltage. The discharge quenching and the restoration of the APD biasing voltage are necessary to enable another photon detection. The article presents the third version of the single photon detecting system made in Romania, the main technical requirements for the included subsystems, measuring methods and experimental results.

Key words: single photon counting, single photon detectors, entangled photons.

1. INTRODUCTION

Quantum technologies emerged recently as the “second quantum revolution” [1] and are subject of many EU-funded research networks such as QUROPE and QUANTIP.

The entanglement, a pure quantum property, is the fundamental brick for the very large field of the quantum information. Applications areas like: quantum teleportation, quantum communication, quantum key distribution keep on developing exponentially *versus* time [2]. Any experimental setup in the above mentioned fields includes a single photon detecting system [3].

The observations on our previous models for single photon detector [4] revealed the need to improuve certain parameters. Thus, the linear measuring range and the detection efficiency were increased. The dark counting rate and sensitivity to mechanical tolerances of the optical fibers used for coupling the instrument to the optical field were reduced. A new method to measure the after-pulsing was found and used to trim the APD’s bias voltage to the specific user’s

requirement: maximum detection efficiency, minimum afterpulsing rate or maximum measuring range. The principle of the adopted solutions and the measured characteristics of our new single photon detector are reported.

During the manufacturing of a small lot (4 pieces), the specific technological procedures were applied and improved; the detecting and measuring system is ready for multiplication.

2. MEASURING SETUP

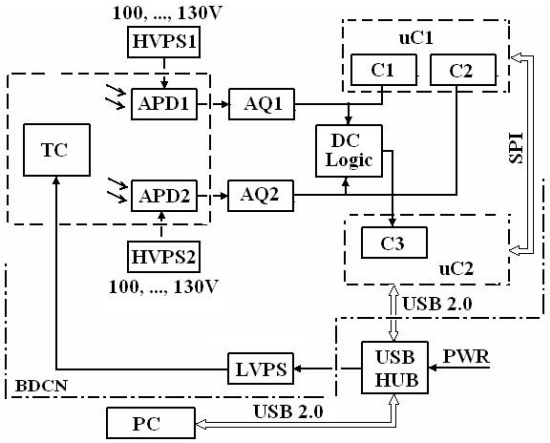

Fig. 1 – Measuring setup: APD1, APD2 – avalanche photodiodes; TC – temperature controller; HVPS1, HVPS2 – high voltage power supplies; AQ1, AQ2 – active quenching circuits; DC Logic – direct coincidence logic circuit; C1, C2, C3 – counters; uC1, uC2 – microcontrollers; LVPS – low voltage power supply; PC – personal computer [4].

The APD1 and APD2, type S9717, are placed inside a thermostat whose temperature is regulated by the temperature controller, TC (Fig. 1). The high voltage power supplies, HVPS1, HVPS2, and the active quenching circuits, AQ1, AQ2, assure the proper working conditions (from electrical point of view) for the APDs. Consequently, an absorbed photon in the active volume of the APD initiates an avalanche discharge. This generates a current pulse high enough to be detected. A little bit latter, the avalanche is quenched by the corresponding quenching circuit. The voltage pulses supplied by the AQ1, AQ2 are registered by the corresponding counter C1 or C2. The direct coincidence logic circuit, DC Logic, detects any pulse pair whose rising edges are inside the coincidence window time; their number is accumulated in the C3 counter. The microcontrollers uC1, uC2 are used both to implement the counters and to assure the communication through serial buses. The acquisition time is determined by the operator and introduced into

the personal computer, PC, through an application specific graphical interface. The measuring result is both displayed on its monitor and saved in a .csv file.

2.1. TEMPERATURE REGULATING SUBSYSTEM

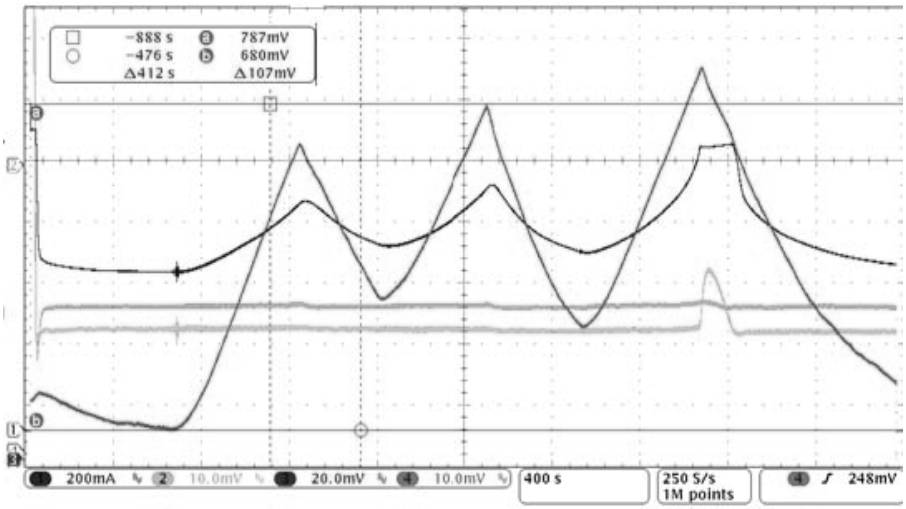

a)

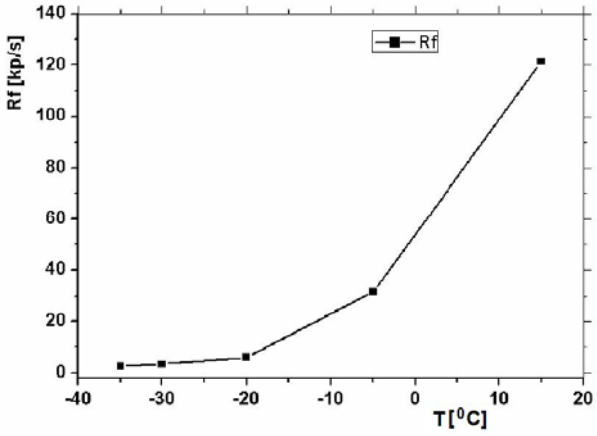

b)

Fig. 2 – a) The time evolution of the: controlled temperature (green line, 1 ^{o}C/div., ch. 4), the heat sink hot point temperature (magenta line, 2 ^{o}C/div., ch. 3), current intensity through the thermoelectric cooler (dark-blue line, 200 mA/div., ch. 1) and voltage across the cooler (light-blue line, 10 mV/div., ch. 2) when the set point temperature equals –30 ^{o}C and ambient temperature is 18 ^{o}C,…, 27 ^{o}C; b) dark count rate, Rf, *versus* working temperature of the APD, when the excess voltage is about 4 V. The extreme values ratio is: 123/2.54 = 47.7.

The temperature regulating system involves both the electronic temperature controller and the rest of the module because all parts are thermally interconnected. More than that, some mechanical parts must obey the constraints imposed by the optical considerations. The time evolution of: regulated temperature when the set point temperature equals –30 ^{o}C, heat think hot point temperature, current intensity through the thermoelectric cooler and voltage across it, under ambient temperature values between 18 ^{o}C,…, 27 ^{o}C, are registered in Fig. 2a; one can estimate the stabilization factor: about 0.01 ^{o}C/^{o}C. The APD's working temperature significantly acts on the dark current rate, as illustrated in Fig. 2b. Also, its stabilization factor value is important to keep a constant detection ratio *versus* laboratory temperature.

2.2. DARK COUNT RATE, AFTERPULSING RATE

The dark count rate depends on the high voltage, too (Fig. 3). There are no pulses for values smaller than 107.5 V; this is the breakdown voltage. In the interval [108.5; 111.5] V, the dark count rate increases linearly against the voltage but, for higher values, the slope of line segments increases. Why? How to choose the right high voltage value?

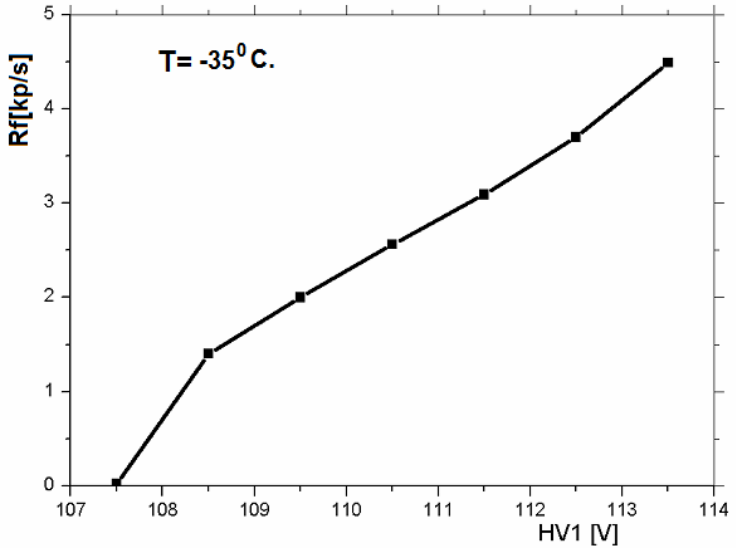

Fig. 3 – Dark count rate *versus* high voltage when working temperature equals –35 ^{o}C.

We've understood that the slope increase is due to the afterpulsing [5]: some free electrons are captured on the impurities from the active volume and initiate a new avalanche close to the moment when the quenching voltage is cut off. So, a

small time interval – less than 1 μs between successive pulses is a signature of the afterpulsing. More than that, the voltage pulses across the APDs we are using are twice larger than ordinary pulses (Fig. 4). This are the two criteria to identify the after-pulses for the APD type S9417 [6]. (The method validity has to be tested for other APD types.)

By using the suggested method, we measured the ratio afterpulsing rate/ dark count rate *versus* the biasing (high) voltage and quenching time (Fig. 5). If the value of these ratios are specified, one can easily determine the maximum high voltage value and the minimum quenching time.

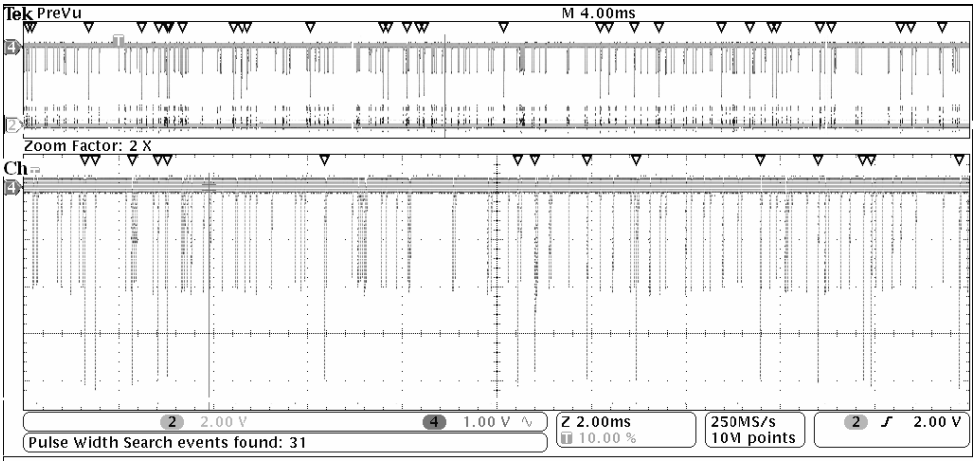

Fig. 4 – Measuring the rate of the after-pulses: the triangles mark them.

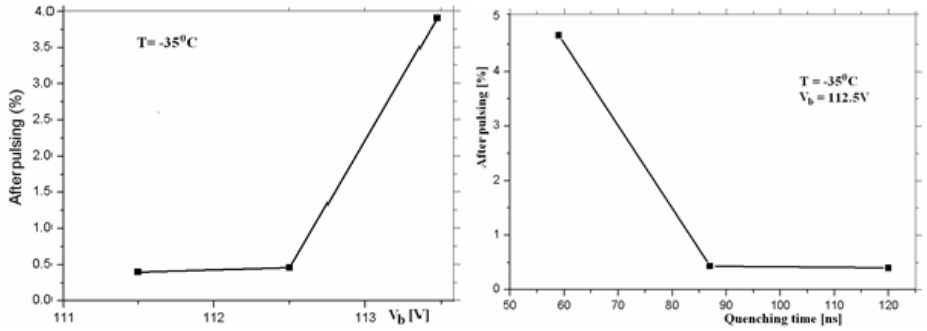

a) b)

Fig. 5 – The ratio afterpulsing rate/dark count rate *versus*:
a) the biasing voltage; b) the quenching time.
Therefore, a single photon detector can be trimmed according
to the application specific requirements.

2.3. OPTICAL SUBSYSTEM

The optical subsystem ensures both the optical coupling of the APD to the field to be measured and isolation against the ambient light.

The female FC connector (Fig. 6) allows the coupling of a multimode optical fiber. The aspheric lens L1 transforms the input divergent light beam into a parallel one, whereas L2 focalizes it on the active area of the APD. The tube OT is necessary to thermally isolate the APD subassembly from the front panel. In principle, this solution fulfils the desired requirements.

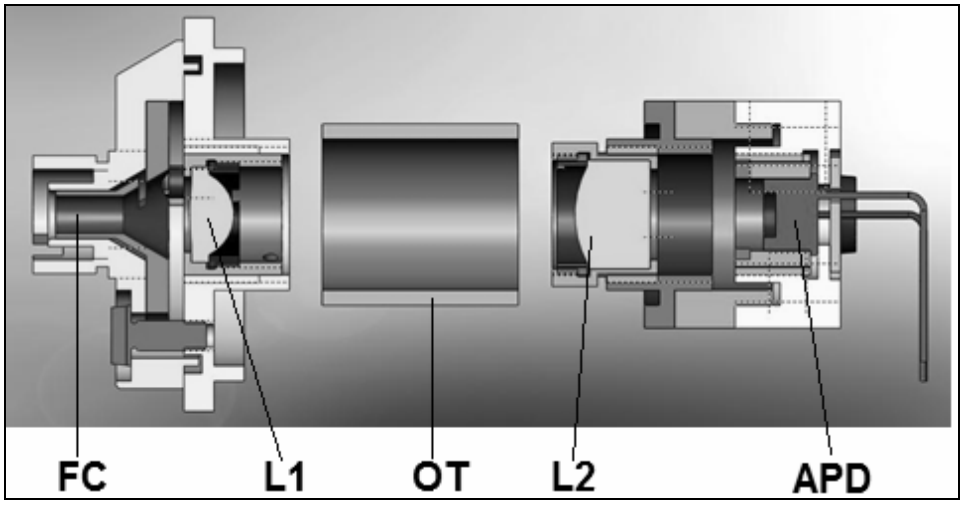

Fig. 6 – A preliminary version of the optic system: FC – female FC connector; L1, L2 – aspheric lenses; OT – optical tube; APD – avalanche photodiode.

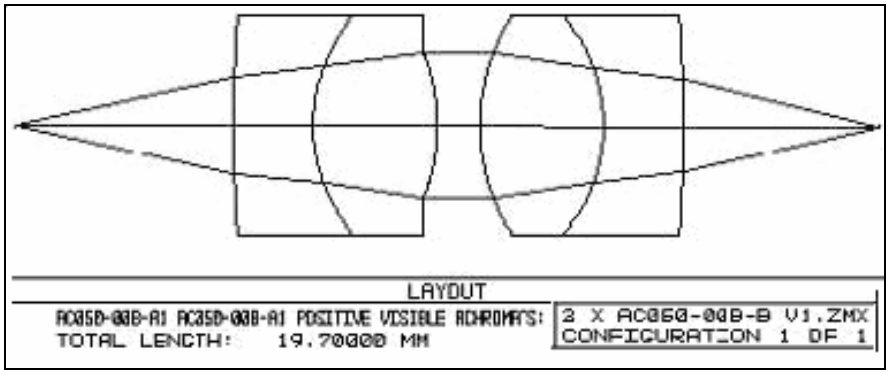

a)

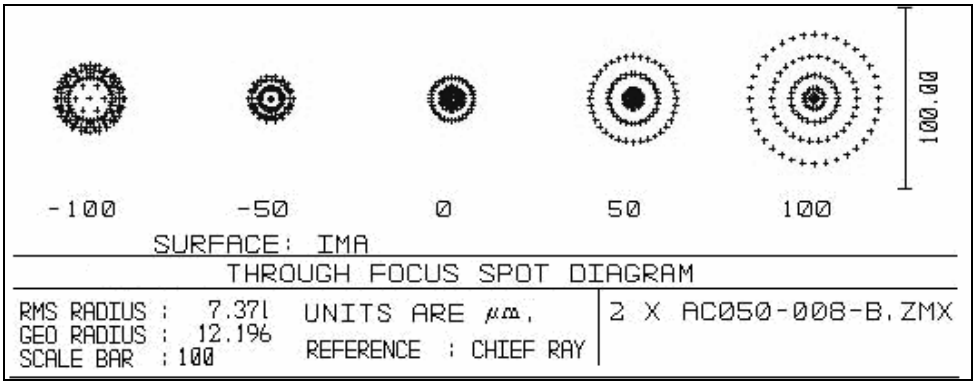

b)

Fig. 7 – The new optic design: a) layout; b) through focus spot diagram.

In practice, it is not acceptable at least for the following reasons:

- a new patch cord will have a slightly different ferule length than that used during L1 position trimming and, consequently, the light coupling factor changes;
- trimming of the L2 position is almost impossible because of the L2 mount tilting;
- cold branch of the thermal circuit has a large outer area witch drastically limits the minimum achievable temperature or, even worse, the thermal system oscillates.

A new solution was designed and tested. The use of achromats instead of the aspheric lenses create a rather tolerant system to the axial positioning errors (Fig. 7): though an + 0.1 mm error in the APD's axial position produces a spot diameter increase from about 0.015 mm to 0.1 mm, nevertheless this value is only half of active area diameter.

A special attention was paid to characterize the incident beam on the APD because any lost optic power reduces the overall single photon detection ratio. A trimmed subassembly (without the APD), connected to a patch cord having on the other end a red light emitting diode, was mounted on an optical bench and brought near a beam profiler. When the minimum spot position was determined, we shot its picture (Fig. 8a) through a microscope objective and analyzed it. The results can be seen in the Figs. 8b–e and allow to visualize the beam and measure its dimensions; the conversion constant from pixel to micrometer was prior determined. The designed parameters were acceptably confirmed.

For the final test, the beam profiler was replaced by an actual APD, prior connected to a current to voltage converter. Then, we measured the output voltage (proportional to the received optical power) *versus* radial position of the focalized

beam; the axial distance is a parameter. The obtained graphs (Fig. 8f) are, practically, superposed: ± 150 μm axial error (corresponding to ± 3 experimental h units) does not affect the response! The plateau of the graphs minima (correspond to the maximum received power) proves that the sensitive area diameter is larger than the beam. Shortly: the adopted solution is a good one.

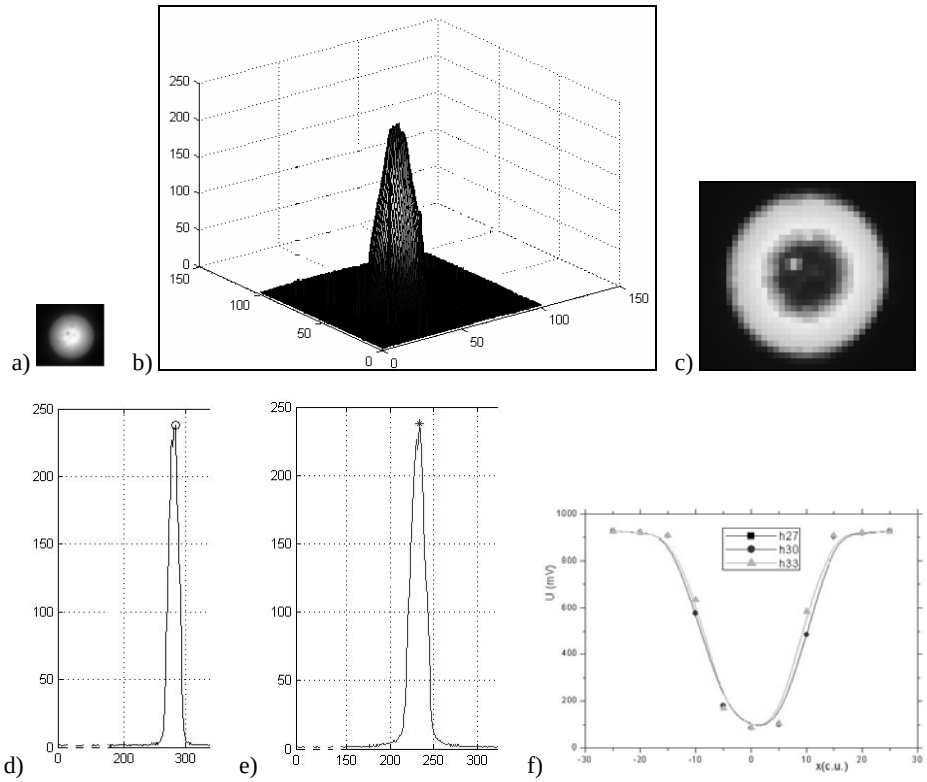

Fig. 8 – Measuring results on the focalized beam: a) the minimum incertitude spot viewed through a microscope objective; b) three dimensional graph of the beam intensity; c) beam intensity projection on xOy plane; d), e) plane sections through the point of maximum intensity; f) the response of a current to voltage convertor connected to the APD, *versus* the radial position of the focalized beam; the axial error is a parameter; the lines are for guide only. One conventional unit: 1c.u. = 12.5 μm.

2.4. APPLICATION SOFTWARE

The application software includes both the firmware installed on microcontrollers and the software resident on the PC. It allows acquisition time setting, counters' reading, data storing, assures graphical interface and generate friendly reports. The graphical user interface (Fig. 9) was designed to attach automatically a unique name – "Raport_masurare_data_timp" (Measuring

report_data_time) – to each measuring report, to reserve locations for the operator's notes, to set the measuring time, to display the acquisition results both as total rate (R.T), and net rates (R.N.). Total and net rates standard deviations (S(R.T), S(R.N.)) are also calculated. Besides the rates, the accumulated numbers can be displayed, too.

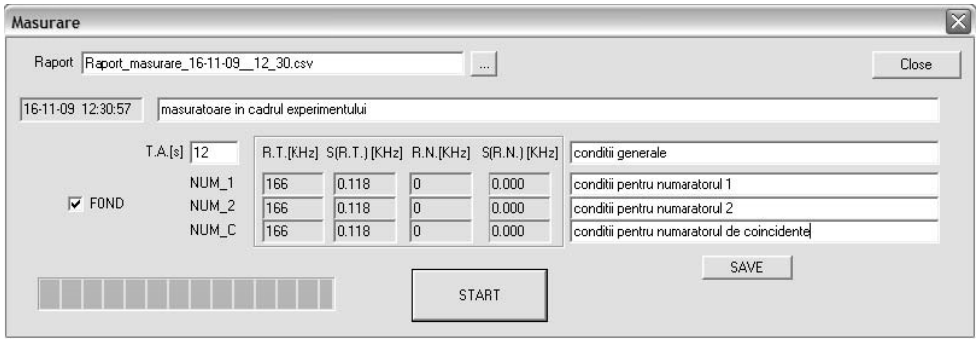

Fig. 9 – The graphical user interface.

2.5. SINGLE PHOTON DETECTING SYSTEM – GENERAL VIEW

The detecting system (Fig. 10) includes: the module type BDCN v3 for single photon detection, coincidence and counting, USB hub capable to supply 5V/3A, application specific software and auxiliaries.

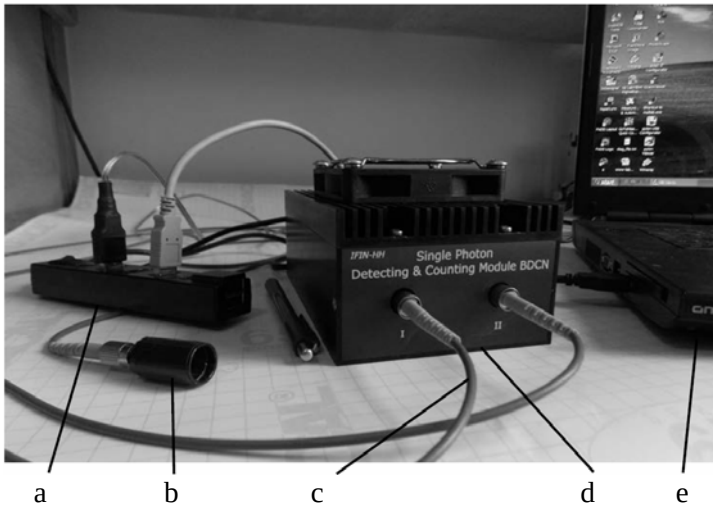

Fig. 10 – Single photon detecting system: a) USB hub; b) optical module; c) patch cord; d) single photon detecting module BDCN v3; e) the associated laptop.

Some relevant characteristics are the following:

- two input channels;
- background rate: < 1 kp/s when the detection ratio = 5%;
- overall detection ratio: at least 30% for afterpulsing rate < 0.5%, wavelength 800 nm;
- direct coincidence window: 4.5 ns, can be lowered to 1 ns;
- dead time: 120 ns;
- linear measuring range: [0.1; 2000] kp/s when acquisition time = 4 s;
- spectral range: (400; 900) nm;
- command and control through an application specific graphical user interface;
- thermal stabilization of the APD at the temperature: –30 ^{o}C;
- working temperature range [0; 30] ^{o}C;
- power: 220 V, 50, …, 60 Hz, 80 VA;
- dimensions for BDCN v3 module (width × length × height): 100 × × 160 × 65 mm;
- weight: 800 g.

3. CONCLUSIONS

A single photon detecting system version 3, as prototype lot, was designed, manufactured and tested; it can be multiplied.

Acknowledgments. This work was supported by the Romanian Space Agency, contract 108/2013. The authors are grateful to Dr. Dragos Falie for helpful discussions and technical support.

REFERENCES

1. Dowling, J.P., Milburn G.J, *Quantum Technology: The Second Quantum Revolution*, Phil. Trans. R. Soc., **A 361**, 1655 (2003); quant-ph/0206091.
2. M. D. Eisaman, J. Fan, A. Migdall, S. V. Polyakov, Invited Review Article: *Single-photon sources and detectors*, Rev Scie. Instrum., **82**, 071101 (2011); doi: 10.1063/1.3610677.
3. S. Cova, M. Ghioni, A. Lacaita, C. Samori and F. Zappa, *Avalanche photodiodes and quenching circuits for single-photon detection*, Appl. Optics, **35**, *12* (1996).
4. Rusu, Al., Rusu, L., *Visible Spectrum Single-Photon Detection Module*, Journal of Science and Arts, Year 10, **1**, *12*, 143–152 (2010).
5. Sergio Cova, A. Lacaita, and G. Ripamonti, *Trapping Phenomena in Avalanche Photodiodes on a nanosecond Scale*, IEEE Electron Device Lett., **12**, *12*, 685–690 (1991).
6. Rusu Al., Rusu L., *A Method to Precisely Identify the After-Pulses when using the S9717 Avalanche Photodiode*, International Physics Conference, TIM 14 – *Physics without Frontiers*, West University of Timisoara, 20th – 22nd of November, 2014.